

Behavior of composite box bridge girders under localized fire exposure conditions

Gang Zhang^{*1}, Venkatesh Kodur², Weifa Yao³ and Qiao Huang³

¹School of Highway, Chang'an University, Xi'an, Shaanxi 710064, China

²Department of Civil and Environmental Engineering, Michigan State University, East Lansing, MI 48864, USA

³School of Transportation, Southeast University, Nanjing, JiangSu 210096, China

(Received June 6, 2018, Revised November 30, 2018, Accepted December 14, 2018)

Abstract. This paper presents results from experimental and numerical studies on the response of steel-concrete composite box bridge girders under certain localized fire exposure conditions. Two composite box bridge girders, a simply supported girder and a continuous girder respectively, were tested under simultaneous loading and fire exposure. The simply supported girder was exposed to fire over 40% of its span length in the middle zone, and the two-span continuous girder was exposed to fire over 38% of its length of the first span and full length of the second span. A measurement method based on comparative rate of deflection was provided to predict the failure time in the hogging moment zone of continuous composite box bridge girders under certain localized fire exposure condition. Parameters including transverse and longitudinal stiffeners and fire scenarios were introduced to investigate fire resistance of the composite box bridge girders. Test results show that failure of the simply supported girder is governed by the deflection limit state, whereas failure of the continuous girder occurs through bending buckling of the web and bottom slab in the hogging moment zone. Deflection based criterion may not be reliable in evaluating failure of continuous composite box bridge girder under certain fire exposure condition. The fire resistance (failure time) of the continuous girder is higher than that of the simply supported girder. Data from fire tests is successfully utilized to validate a finite element based numerical model for further investigating the response of composite box bridge girders exposed to localized fire. Results from numerical analysis show that fire resistance of composite box bridge girders can be highly influenced by the spacing of longitudinal stiffeners and fire severity. The continuous composite box bridge girder with closer longitudinal stiffeners has better fire resistance than the simply composite box bridge girder. It is concluded that the fire resistance of continuous composite box bridge girders can be significantly enhanced by preventing the hogging moment zone from exposure to fire. Longitudinal stiffeners with closer spacing can enhance fire resistance of composite box bridge girders. The increase of transverse stiffeners has no significant effect on fire resistance of composite box bridge girders.

Keywords: bridge fires; fire resistance; steel-concrete composite box girders; fire tests; finite element analysis; bridge girders

1. Introduction

Fire is one of the most severe hazards which built-infrastructure may experience during their service life (Quiel *et al.* 2015, Garlock *et al.* 2012). In recent years, bridge fires have become a growing concern due to rapid urbanization and increased transport of flammable materials. Numerous bridge fire incidents have been documented in the literature (Alos-Moya *et al.* 2014, Aziz *et al.* 2015, Kodur *et al.* 2013, Kodur *et al.* 2017, Naser and Kodur 2015, New York State Department of Transportation 2008, Quiel *et al.* 2015, Zhang *et al.* 2017). In some of these incidents, fires have caused substantial structural damage and in limited cases even full collapse of bridges, leading to significant economic and public losses. Therefore, recent studies are pointing to the need for fire safety provisions in bridges so as to maintain structural stability and integrity in the event of fire. While provision

of fire resistance to structural members is a major design requirement in buildings, there is no such provision for structural members in the case of bridges suffered from different level of fire exposure as per AASHTO and other standards (AASHTO 2007, NFPA 2011).

Over last decades, limited studies on fire resistance of composite beams in buildings have been conducted (Balaji *et al.* 2016, Glassman *et al.* 2016, Nguyen *et al.* 2015, Wang 1998). However, the response of composite bridge girders under fire can be significantly different from that of buildings due to significant differences in fire severity, fire protection, measures geometry of structural member and relevant failure limit states (Alos-Moya *et al.* 2017, Kodur *et al.* 2017). The limited research information reported in literature is based on numerical analysis with regard to experimental data on only fire tests on I-shaped composite bridge girders (Alos-Moya *et al.* 2017, Aziz *et al.* 2015, Kodur *et al.* 2013, Kodur *et al.* 2017, Morbioli *et al.* 2018, Naser and Kodur 2015, Zhou *et al.* 2018). One main conclusion drawn in these studies is that the composite action arising from steel-girder-concrete-slab interaction can significantly enhance fire resistance of composite

*Corresponding author, Professor
E-mail: zhangg_2004@126.com

girders of a steel bridge girder. Results from literature (Alos-Moya *et al.* 2017, Aziz *et al.* 2015, Kodur *et al.* 2013, Kodur *et al.* 2017, Naser and Kodur 2015, Zhou *et al.* 2018) show that time to failure and mode of failure in fire exposed steel I-shaped girders is highly influenced by web slenderness, spacing of stiffeners, type of fire exposure, fire position and prestress level in external tendons, and failure mode of I-shaped steel girders changes from flexural yielding to web shear buckling when web slenderness in girders exceeds 100.

Composite box girders sections are commonly used in long-span bridges because of their high torsional resistance as compared to I shaped girder sections (Cheng *et al.* 2016, Kim *et al.* 2015, Nie *et al.* 2011, Zhu *et al.* 2017). In the last decade, some simply supported composite box bridge girders have been designed to surpass 40 m span (even 60 m), or multi-span continuous girders, with spans have exceeding 110 m, have been adopted in practice. Therefore, assuming a constant fire load along the long-span bridge for the entire span is probably not the most realistic fire scenario (Alos-Moya *et al.* 2017, Quiel *et al.* 2015). These long span composite box bridge girders are likely to experience localized fire exposure condition over partial span of the girder. Currently, there is a lack of data on fire performance of steel-concrete composite box bridge girders (Erdem 2017, Pantousa *et al.* 2017, Tang *et al.* 2017, Zhou *et al.* 2018). To overcome this knowledge gap, experimental and numerical studies on steel-concrete composite box girders is carried out by subjecting the girders to localized fire exposure conditions. Detailed results on the response of composite box girders under different fire exposure conditions are presented in this paper.

2. Experimental program

The experimental program consisted of fire resistance tests on two steel-concrete composite box bridge girders, in which one is simply supported and the other is continuous. These two girders were tested to investigate the behavior under combined effects of structural loading and localized fire exposure.

2.1 Fabrication of test specimens

The tested bridge girders comprised of an open box steel section (U-section) girder supporting a reinforced concrete slab. These two composite girders were designed as per GB 50917 provisions (GB 50917 2013). The main variable in these two test specimens was the support conditions. The first test girder was simply supported (CG1), while the second girder was supported as a two-span continuous girder (CG2). The span length of girder CG1 was 3.4 m, while the two-span girder had lengths of 2.4 m and 2.0 m in the 2 spans. The various sectional dimensions, of the box girder and slabs are given in Table 1 and also in Fig. 1.

The concrete slab was designed to be of 100 mm thick placed over the steel box girder. Four rows of 20 mm diameter shear studs were welded within webs to maintain full composite action between the steel box girder and the concrete slab, as shown in Fig. 2. The concrete slab was

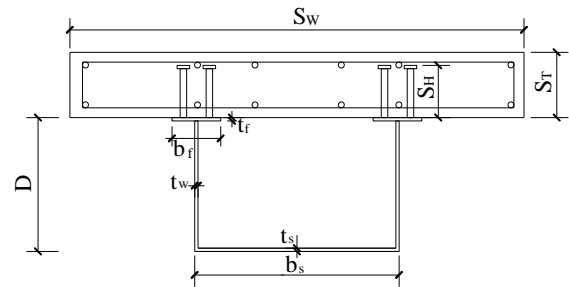


Fig. 1 Sectional dimensions of the composite box girder

Table 1 Parameters related to sectional geometry, structural system and applied load of tested girders

Parameter	Description	Girder CG1	Girder CG2
Sectional geometry	Span distribution (between supports), mm	3400	2400/2000
	Total length (end to end), mm	3800	4800
	Flange plate ($b_f \times t_f$), mm	75×5	75×5
	Web plate ($D \times t_w$), mm	195×5	195×5
	Bottom slab ($b_s \times t_s$), mm	320×5	320×5
	Width of concrete slab (S_w), mm	700	700
	Thickness of concrete slab (S_r), mm	100	100
Structural system	Height of stud (S_H), mm	80	80
	Simply supported or continuous	Simply supported	Continuous
Capacity at ambient temperature	Mid-span Flexural (composite), kN.m	150	150/150
	Negative flexural of pier top (composite), kN.m	-	85
Applied load	Applied load, kN	40/40	70/60
	Applied flexural/mid-span flexural capacity	40%	20%/11%
	Applied flexural/Negative flexural capacity of pier top	-	40%
Fire exposure location (ISO834)		40% span length in the mid portion	38% length of the 1st span and full length of the 2 nd span



Fig. 2 Fabrication procedure of composite girders

reinforced with two layers of tension steel reinforcement at the bottom and top sides cycled with stirrups. In addition, a transverse diaphragm with 5 mm thick was set in the hogging moment zone on the top of pier to increase the capacity of resisting local buckling.

2.2 Instrumentation

The instrumentation mounted on the girders comprised

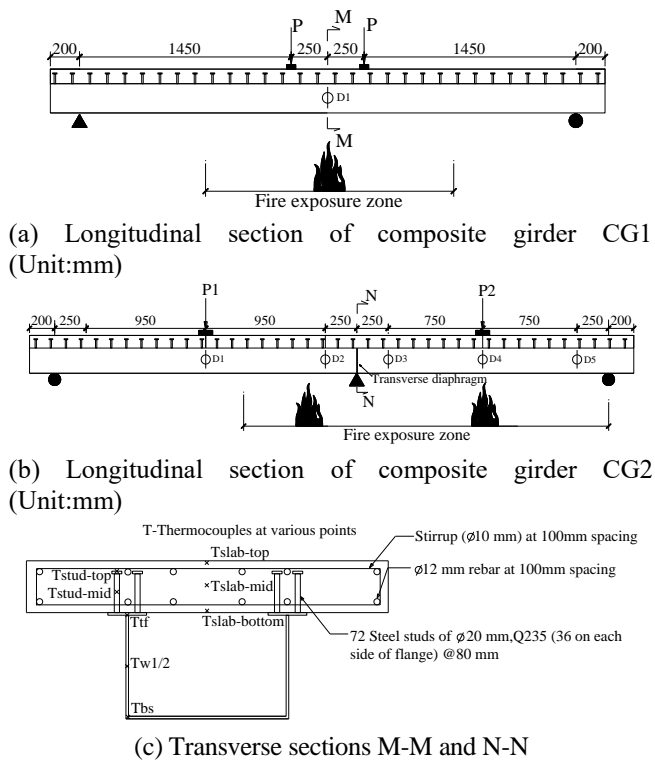


Fig. 3 Instrumentation layout of composite girders CG1 and CG2

of thermocouples to measure cross sectional temperatures, and transducers to measure deflections.

K-type thermocouples were placed at mid-span section of girder CG1 and pier top section of girder CG2. Thermocouples were installed at bottom slab, web, top flange, shear studs and at different depths in concrete slab at each section of tested girders to measure progression of sectional temperature during the fire test, as shown in Fig. 3. The mid-span deflection of tested girder CG1 was measured using one displacement transducer placed on the top of concrete slab. Five displacement transducers were mounted on girder CG2 to measure deflections in each section (See Fig. 3). Locations D1 and D2 selected in the first span were used to measure the mid-span deflection and the hogging moment zone deflection respectively. The rate of deflection in locations D1 and D2 was compared to investigate the failure time of the hogging moment zone under localized fire exposure conditions. Locations D3, D4 and D5 selected in the second span were utilized to measure the deflection in the hogging moment zone, the mid-span and the span end. Locations D3 and D5 were symmetric about the center of the second span. The rate of deflection in locations D3 and D5 was also compared to investigate fire resistance of the hogging moment zone.

2.3 Test setup and procedure

Fire tests on composite girders were conducted in a specially built fire testing furnace. The furnace and the actuator set-up allow simultaneous application of both fire and structural loading on test specimens to simulate conditions experienced by a structural member during a fire event. The

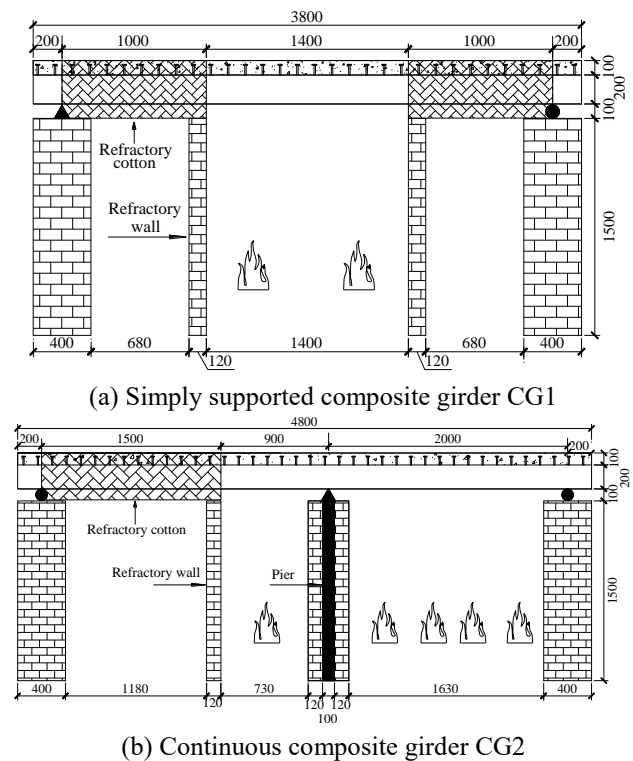


Fig. 4 Schematic of test set-up for testing composite girders under localized fire conditions

interior dimension of the heating furnace is $4.0\text{ m} \times 4.0\text{ m} \times 1.5\text{ m}$. During fire tests, fire temperatures within the furnace were continuously monitored using six thermocouples distributed spatially inside the furnace. The failure state was observed using the preinstalled observation window.

All sides of the composite girder assembly except the top side of the concrete slab were exposed to ISO834 fire conditions (ISO 1999) due to no provisions specified fire scenarios on bridge structure in current code and standards (AASHTO 2007, NFPA 2011, Kodur *et al.* 2017). The fire exposure length in CG1 was 1.4 m of the middle zone of girder. The non-fire exposed length of the girder was insulated with thick refractory cotton insulation, and two refractory walls were built to prevent fire radiation to that portion of the girder.

To investigate the failure mode of continuous bridge box girder under certain localized fire condition, the fire was put near the support of continuous girder. Thus, in girder CG2 length of 0.9 m in the first span (adjacent to pier top) and the entire second span were exposed to fire, as shown in Figure 3. The particular fire scenario specified in CG2 was utilized to compare the deflection progression at different locations in each portion under local fire exposure condition and entire span fire exposure condition.

Girder CG1 was subjected to a dual point loading of 40 kN, equivalent to 40% of its flexural capacity at room temperature, and each point load was applied at 0.25 m from center side of mid span. A triangle solid steel and a round steel column were used to simulate simply supported end conditions, where the height of the triangle solid steel and the diameter of the round steel column were both 100 mm, as shown in Fig. 4(a). Girder CG2 was subjected a single point

Table 2 Properties of Q235 steel and concrete used in fabrication of composite girders

Steel	f_y (MPa)	f_u (MPa)	Strain at f_u	Elastic modulus (MPa)
	238.9	438.4	0.327	203,529
Concrete	Age (d)	Compressive strength (f_c , MPa)	Indirect tensile strength (f_t , MPa)	Elastic modulus (MPa)
	28	26.6	2.9	32,086



Fig. 5 Picture showing of the testing girder

load at mid-span of each span, and the loads were 70 kN and 60 kN respectively, representing 40% of room temperature flexural capacity. To simulate the hinge-bearing and sliding-bearing support conditions in continuous composite girder, a triangle solid steel was located on the pier top and two round steel columns were installed at both ends, where the height of triangle solid steel and the diameter of the round steel columns were 100 mm, as shown in Fig. 4(b).

The loads applied on each girder were gradually increased by incrementing hydraulic pressure in the actuator 30 minutes prior to fire exposure. The load was kept to stabilize about 60 minutes after the target load was reached, as shown in Fig. 5. Then, the furnace was turned-on and the furnace temperature was controlled to follow ISO834 time-temperature exposure (ISO 1999). The loading on the girder was kept at the specified level on the girder during the fire test. When the deflection in the girder exceeded $L/30$ (where L was the span length), or when the girders were unable to resist the applied loading, the fire exposure was stopped.

2.4 Material properties

The box girder was fabricated with Q235 steel, commonly used in steel and composite bridge construction (Zhang *et al.* 2017). The slab was made of silicate concrete. To evaluate mechanical properties of steel and concrete used in fabrication of the composite girder assemblies, strength tests were carried out on steel coupons and concrete prisms. Three coupons cut from girders were tested to evaluate tensile strength of steel. For evaluating concrete strength, concrete prisms were cast from concrete batch mix during fabrication of respective slabs. As per GB 50917 provisions (GB 50917 2013), three concrete prisms (300 mm×150 mm×150 mm) were tested on 28 day to evaluate compressive strength and tensile strength.

In addition, three concrete prisms were tested to evaluate room temperature elastic modulus of concrete. A summary of results of mechanical properties of steel and concrete is tabulated in Table 2.

3. Results

Data generated from fire tests is utilized to evaluate comparative response of two box girders under localized fire conditions. Thermal response, structural behavior, as well as failure modes, are compared to illustrate the comparative fire behavior of composite girders.

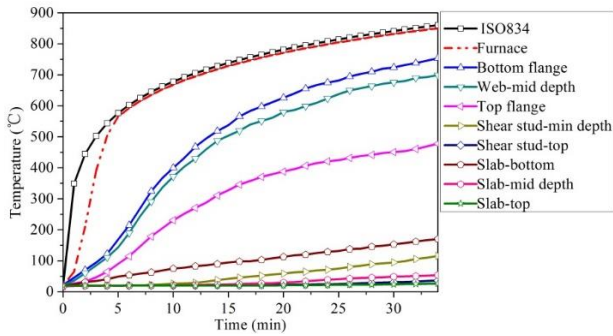
3.1 Thermal response

Girders CG1 and CG2 were exposed to ISO834 fire exposure (ISO 1999) in each test. The measured temperature-time curves at various cross-sectional locations in each girder are shown in Fig. 6. It can be seen from Fig. 6 that top flange in each box girder has much lower temperature as compared with bottom flange throughout the fire exposure duration. This is mainly attributed to the fact that the concrete slab provides insulating effect to the top flange of the steel girder and concrete due to its higher thermal capacity and lower thermal conductivity properties can absorb much of the heat from the top flange. Also, the top flange is not directly exposed to fire.

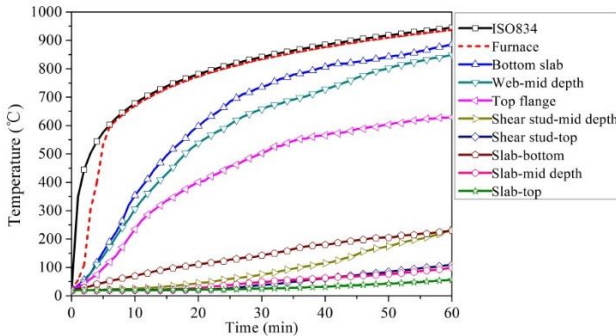
Shear studs present in the composite girder experience much lower temperatures as compared with the top flange temperature. This is due to the fact that the shear studs are embedded in concrete and concrete slab, acting as heat sink, absorbs much of the heat from studs. Temperatures in concrete slab are much lower than that in steel web, and this produces significant thermal gradients along the depth of the composite girder section. These gradients induce thermal stresses which in turn influence structural behavior of fire exposed composite girders.

3.2 Structural response

The structural response of composite girders can be evaluated by tracing progression of deflection as a function of fire exposure time. Fig. 7 shows progression of mid-span deflection in girder CG1 plotted as a function of fire exposure time. The deflection response in the girder can be grouped under three stages. In Stage 1 (initial 15 minutes), mid-span deflection increases linearly with time and this deflection mainly results from high thermal stresses and associated curvature developed within the girder section arising from high temperature gradients. In stage 2 (from 15 min to 25 min), the pace of deflection increases and this deflection is mainly due to temperature induced deterioration in strength and modulus of steel. In final stages, after 25 min of fire exposure, when steel temperature in bottom slab and lower parts of web exceeds 600°C, mid-span deflection increases rapidly. This is mainly attributed to the fact that the plasticity of steel spreads further in the web and bottom flange and the concrete slab in mid-span experiences crushing, leading to formation of a plastic hinge at the mid-span. When the mid-span deflection in girder reaches $L/30$ the girder is said to attain failure and this occurs at 33 min into fire exposure.



(a) Composite girder CG1



(b) Composite girder CG2

Fig. 6 Measured temperature profile in girders CG1 and CG2 as a function of fire exposure time

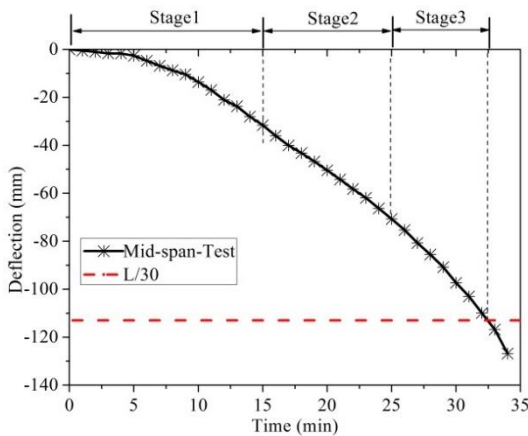
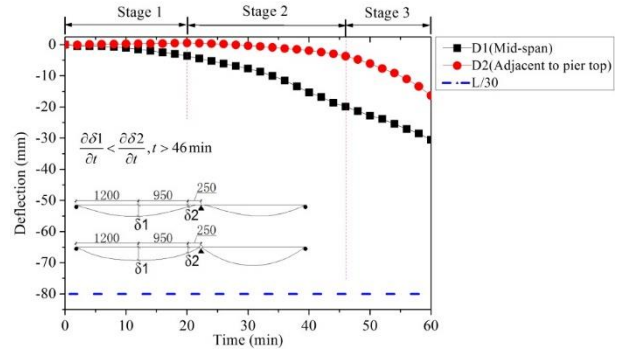
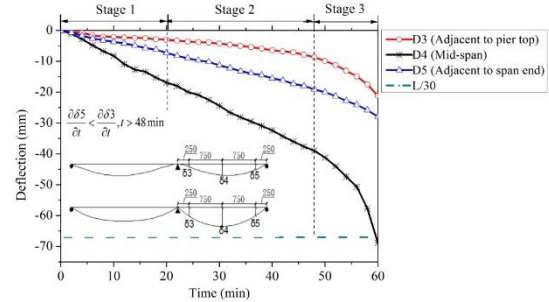


Fig. 7 Progression of deflection in girder CG1 with fire exposure time

Fig. 8(a) shows the deflection progression in span 1 of composite girder CG2 plotted as a function of fire exposure time. The deflection response plotted corresponding to locations D1 and D2 on girder CG2 (shown in Fig. 3(b)) can be grouped under three stages. In the initial stage of fire exposure (up to 20 min), deflections at locations D1 and D2 increase slowly mainly caused by the thermal bowing resulting from high temperature gradient developed between the bottom flange and web and concrete slab of the girder section. At this stage, though strength and elastic modulus of steel and concrete reduce slightly, the structural stiffness of composite box girder in this span remains almost unchanged this is mainly attributed to the fact only less than 40% of the span is exposed to fire, and also location D2 is located in the hogging moment zone. In the next stage of fire exposure



(a) span 1 in composite girder CG2



(b) span 2 in composite girder CG2

Fig. 8 Details of PC box scaled model girder

(between 20 and 46 min), deflections at locations D1 and D2 increase slightly due to the considerable reduction in strength and stiffness properties of steel in fire exposure zone. In the final stage of fire exposure (after 46 min), deflection at location D2 increases with a more rapid pace than that at location D1, this is mainly contribute to the fact that the web and bottom flange adjacent to the pier top experiences significant buckling resulting from lower initial bending capacity and faster degradation of bending capacity during fire exposure. Thus, the function of the hogging moment zone fails and the two-span continuous composite box girder has transformed into two simply composite box girders.

The deflection progression at locations D3, D4 and D5 (See Fig. 3(b)) in span 2 of girder CG2 plotted as a function of fire exposure time is shown in Fig. 8(b). During the early stage of fire exposure (up to 20 min), deflections at all locations increase gradually with fire exposure time. The initial deflections are mainly caused by high temperature gradients through the girder section and the slight reduction in elastic modulus of steel resulting from the elevated temperature in the girder section. Between 20 and 48 min, the rate of deflection increases more quickly due to faster degradation of strength and stiffness in steel at high temperatures. After 48 min, generally deflection in each location increases rapidly due to the spread of plasticity and the effect of high-temperature creep. As shown in Fig. 3, locations D3 and D5 were symmetric about the center of the span, and located in the hogging moment zone and the positive moment zone respectively. The rate of rise in deflection at location D3, within the hogging moment zone, is lower than that at location D5 in the positive moment zone. However, the deflection in the hogging moment zone increases at a faster pace than that in the positive moment zone towards final failure stage. This behavior is mainly due



(a) Composite girder CG1



(b) Composite girder CG2

Fig. 9 Illustration of failure patterns in CG1 and CG2 after exposure to localized fire

Table 3 Summary of the test results in composite girders CG1 and CG2

Description	Composite girder CG1	1 st span of composite girder CG2	Hogging moment zone	2 nd span of composite girder CG2
Failure limit state	Deflection limit ($L/30=113$ mm)	Deflection limit ($L/30=80$ mm)	Buckling in the web and bottom flange	Deflection limit ($L/30=67$ mm)
Failure time of each portion (min)	33	No failure	46	60
Failure time of overall structural system (min)	33		46	

to bending buckling of the web and bottom flange in the hogging moment zone, which leads to failure of continuous structure.

3.3 Failure modes

A number of observations were made during the fire tests and also after completion of fire tests to capture changes in behavior and also failure modes in the two composite box girders. These observations, together with recorded temperature and deflections, are utilized to identify progression of crushing and cracking, buckling and failure modes in both composite girders.

Fig. 9(a) illustrates failure pattern and extent of deformation in the simply supported composite girder CG1. During the initial stage of fire exposure, a large amount of

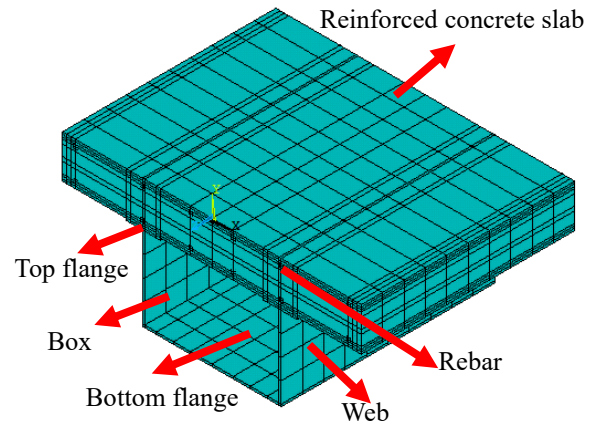


Fig. 10 3-D discretization of girder cross-section for thermal analysis

water vapor from the concrete escaped with the rise in temperatures in the slab. At 33 min, this girder experienced significant degradation in flexural capacity (See Fig. 7) and thus failed, which resulted from yielding at the bottom flange and severe crushing in the concrete slab. When the tested simply girder were exposed to fire, the neutral axis of the composite box section moved upward due to degradation of steel strength of the web and bottom flange at elevated temperature. The neutral axis was located in the concrete slab at failure stage. Hence, test observations indicated no buckling in the web and bottom flange due to the fact that the web and bottom slab was located in tension region when the tested girder approaching failure at elevated temperature. The girder formed a V shape at failure stage due to large deflections, large rotations at the girder span ends and also severe crushing of concrete at the mid-span zone.

The failure pattern and extent of deflection in the composite girder CG2 after fire exposure are illustrated in Fig. 9(b). The composite girder CG2 experienced significant bending buckling in the web and bottom flange as well as severe transverse cracking in the concrete slab in the hogging moment zone. When the tested continuous girder was exposed to fire, the neutral axis of the composite box section in the hogging moment zone moved upward due to degradation of steel strength of the web and bottom flange at elevated temperature. At the failure stage the neutral axis moved into the concrete slab, and the web and bottom flange in the hogging moment zone was mainly located in longitudinal compression region, thus vulnerable to significant bending buckling in the web and bottom flange under fire conditions. The fire-damaged features in the positive moment zone of the continuous composite box girder CG2 were similar to that of the composite girder CG1.

A summary of the test results, including failure time and failure modes, is summarized in Table 3. Failure time of girder CG1 with simply supported ends is dependent on failure limit state of deflection. For composite girder CG2 with continuous supports, no failure occurs in the first span and failure occurs in the second span at 60 min depending on deflection limit. However, the fire resistance of the hogging

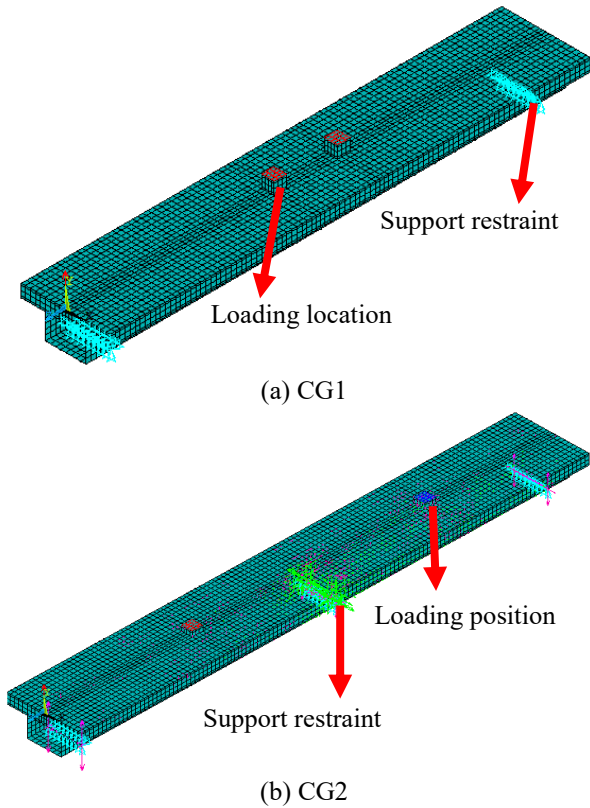


Fig. 11 Three-dimensional discretization of bridge girder for structural analysis

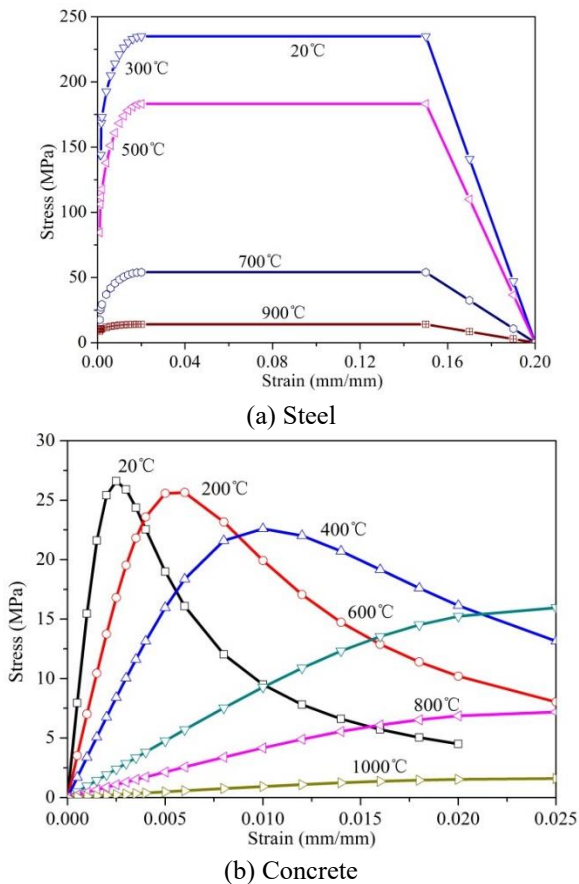
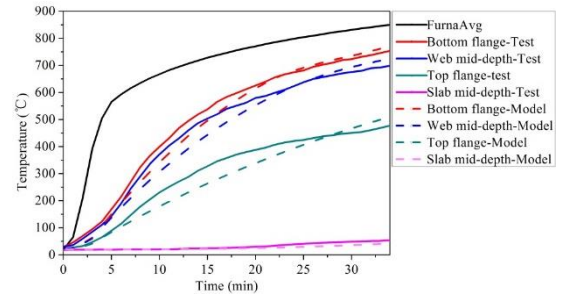
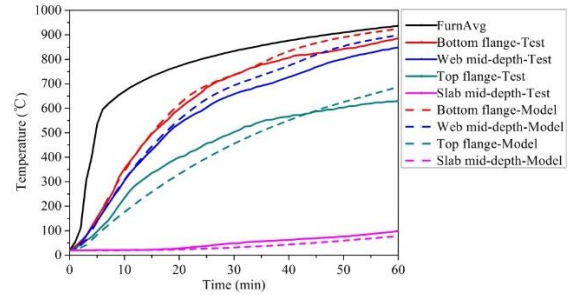


Fig. 12 Stress-strain relations of material at different temperatures (CEN 2004)

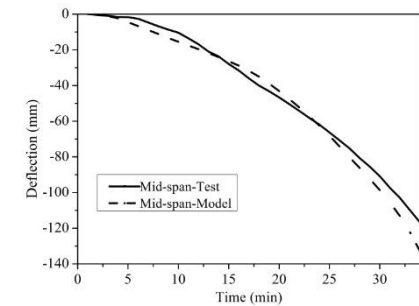


(a) Composite girder CG1

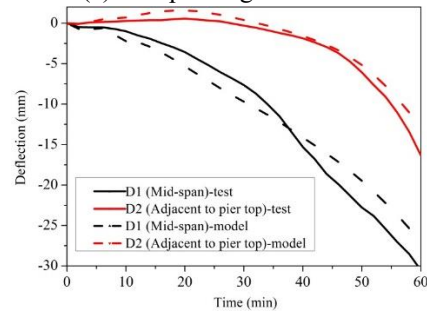


(b) Composite girder CG2

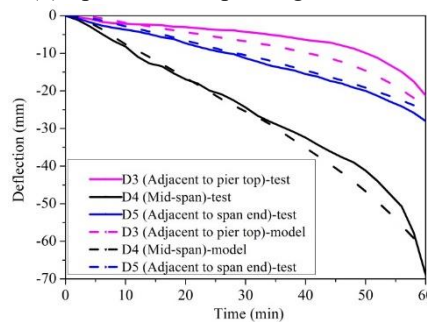
Fig. 13 Comparison of predicted and measured cross-sectional temperatures in CG1 and CG2



(a) Composite girder CG1



(b) Span 1 of composite girder CG2



(c) Span 2 of composite girder CG2

Fig. 14 Comparison of predicted and measured deflection in composite girder CG1 and CG2

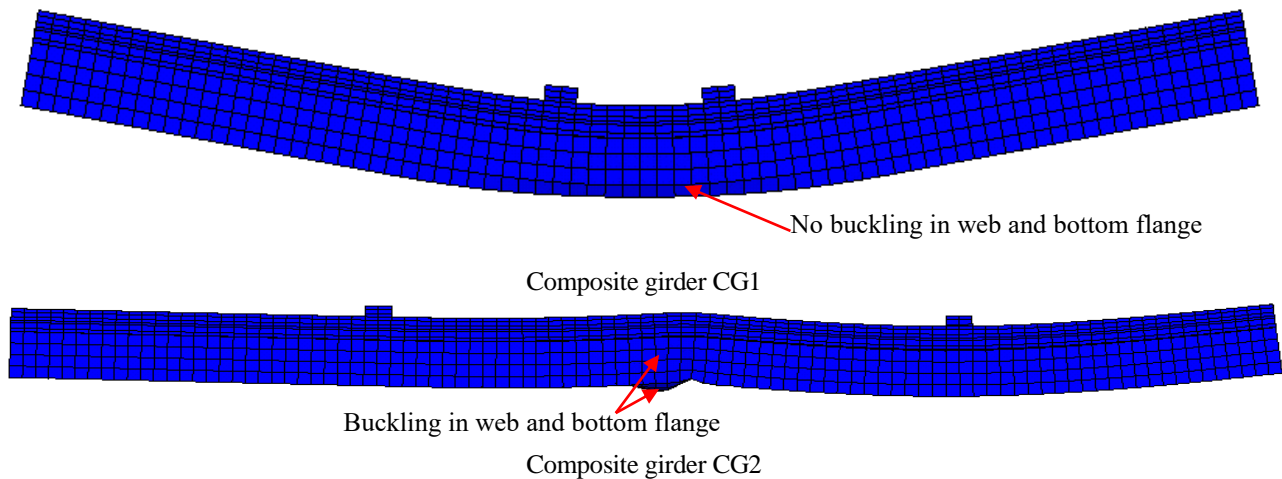


Fig. 15 Predicted failure patterns at failure time by ANSYS in composite girders CG1 and CG2

moment zone fails in 46 min, earlier than failure time in mid-span of span 2, this is due to significant buckling of the web and bottom flange in the hogging moment zone. Therefore, fire resistance of the continuous composite box bridge girder is highly dependent on the onset of temperature induced buckling in the hogging moment zone (close to interior supports).

4. Numerical studies

The above data from fire tests was utilized to validate a finite element model developed in ANSYS (ANSYS 2013) to trace the response of fire exposed composite girders. The analysis was carried out in two stages; thermal and structural analysis. The modeled composite girder, comprised of different structural components, namely, steel girder with reinforced concrete slab on top. The thermal-analysis results were applied uniformly as a thermal-body load on the structural model along the fire exposure zone. High-temperature thermal and mechanical properties of steel and concrete were provided as input into the analysis. Strength limit and deflection limit states was also utilized to evaluate failure, namely the girder could no longer remain the specified applied loading as per the service function from the original structural system.

4.1 Discretization for thermal analysis

For thermal analysis, the composite girders were discretized with SOLID70 and LINK33 elements; available in ANSYS (ANSYS 2013). SOLID70 is a 3D element with three-dimensional thermal conduction capability, and is made of eight nodes, with a single degree of freedom at each node, namely temperature. The external surface of SOLID70 elements, that are exposed to fire, except on the top surface of the concrete slab and inside of box girder, simulated the surface effects of convection and radiation that occurred from the fire zone to the composite girder. LINK33, a uniaxial element, has ability to conduct heat between two nodes and utilized to simulate temperatures of rebar in concrete slab.

Additionally, the external surface of concrete slab inside box section, simulated the surface effects was dependent on radiation from steel box girder at elevated temperature. The discretization adopted for the thermal analysis of the composite girder is shown in Fig. 10.

Both convection and radiation were applied to simulate heat transfer from fire zone to boundaries of the composite girder. Convection coefficient $\alpha_c = 25 \text{ W}/(\text{m}^2\text{C})$ was applied for the exposed surface in the thermal analysis as per Eurocode 1 recommendation (CEN 2002). To simulate radiation effect, different values of emissivity factors were applied based on the exposure boundaries (Kodur *et al.* 2017). Due to the different radiation distance of fire resource to the external face of box section, an effective emissivity factor of 0.7 was used for the fire exposed surfaces of the bottom flange, 0.5 was used for the fire exposed surfaces of the web, and 0.4 was used for fire exposed surfaces of the top flange and bottom of the concrete slab outside box girder. The heat in the concrete slab inside box girder was mainly resulted from the radiation of the web and bottom flange at elevated temperature, therefore the emissivity factor 0.2 and 0.3, associated with fire exposure length, was applied for simulating progression of temperature in the concrete slab.

To simulate radiative heat transfer, a Stefan-Boltzmann radiation constant of $5.67 \times 10^{-8} \text{ W}/(\text{m}^2\text{C})$ was applied in the thermal analysis. The thermal properties of steel and concrete, namely thermal conductivity, specific heat and thermal expansion, were provided as input data into ANSYS based on such provisions taken from literature (CEN 2004, CEN 2005, Lie and Denham 1993).

4.2 Discretization for structural analysis

The output from thermal analysis (temperature), was applied as a thermal-body load on structural elements to predict the behavior of fire exposed composite box girders. For structural analysis, the concrete slab of composite girder was discretized using SOLID65 elements, and steel box girder was modeled with SHELL181 elements, and rebar was modeled with LINK8 elements (ANSYS 2013). SOLID65 is defined by eight nodes having three degrees of freedom per

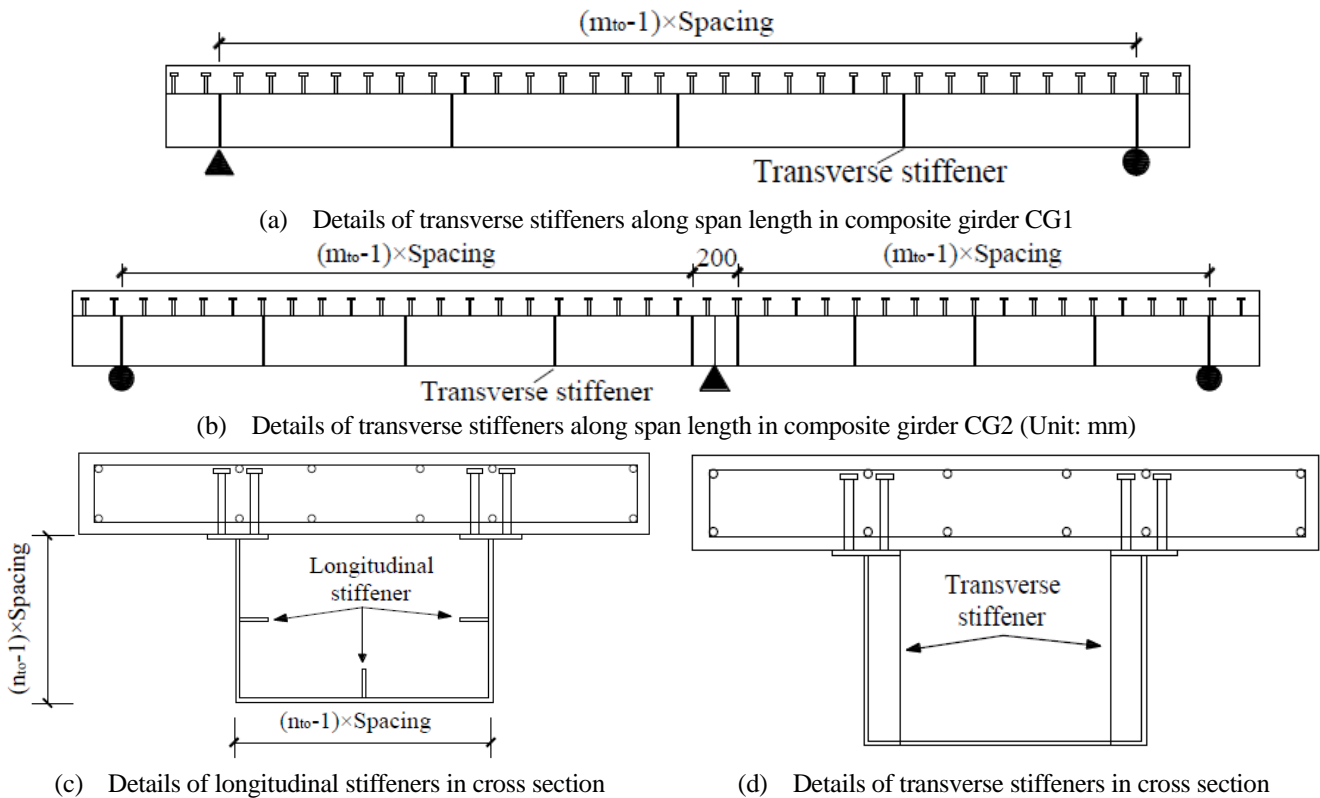


Fig. 16 Layout of stiffeners in composite box girders

node, namely, translations in nodal x , y , and z directions. This element is well-suited to be applied for 3-D modeling of solids with or without reinforcing bars, since it is capable of simulating cracking in tension and crushing in compression, as well as account for plasticity and large strains effects. SHELL181 element is defined by four nodes having six degrees of freedom at each node, namely, three translations in nodal x , y , and z directions and three rotations about x , y , and z -axes. This element is suitable for analyzing thin to moderately-thick shell structures and is capable of capturing local buckling effects in the girder. LINK8 element is a 3-D spar having two nodes with three degrees of freedom, namely three translations in x , y , and z directions. This element can be well used to model rebar with ability of accounting for plasticity, large deflection and large strain effects.

According to test observations during fire tests, assumption of no bond-slip can be used to account for interaction between concrete slab and steel studs, as well as concrete slab and rebar. To account for common action of composite box bridge girder, node-to-node interaction modeled as composite action was utilized to discretize the structural model. The same nodes were shared between the solid elements of the concrete slab and the shell elements of the top flange in the steel girder, and the same nodes were shared between the solid elements of the concrete slab and the link elements of rebar. The 3-D structural model and the meshing and support restraint applied for structural analysis are shown in Fig. 11.

Mechanical properties of concrete and steel were applied as per the specified provisions (CEN 2002, CEN 2004, CEN 2005, Lie and Denham 1993). Stress-strain

relations of concrete and steel are critical for fire-resistance analysis, and these relations vary with temperature. According to Eurocode 2 and 3 provisions (CEN 2002, CEN 2004, CEN 2005), strength data from room temperature tests (See Table 2) were adjusted with relevant reduction factors for generating high temperature stress-strain relations of concrete and steel. Temperature dependent stress-strain relations of steel and concrete taken from literature (CEN 2004) were used in the analysis and are shown in Fig. 12.

4.3 Analysis details

The tested composite girders CG1 and CG2 were analyzed using the above developed model in ANSYS (ANSYS 2013). In the analysis the same conditions of fire exposure, load level and support restraints as in tested composite girders, were simulated.

The fire temperature was input at various times to carry out heat transfer analysis. A 3-D finite element method was applied to perform heat transfer analysis. Following the heat transfer analysis, temperatures generated from thermal analysis were applied as a thermal-body-load on structural elements of the girder to simulate conditions of fire exposure on composite girder.

As part of strength analysis, deflections under applied loading (See Table 1) at room temperature were evaluated at initial (first) time step. For the subsequent time steps, the temperature dependent stress-strain relations were input according to temperature within elements. At each iteration within a time step, Newton - Raphson solution technique was

Table 4 Summary of parametric studies in composite girders CG1 and CG2

Composite girder	Each portion	n_{t_0}	m_{t_0}	Failure limit state	Failure time of each portion (min)		Failure time of overall structural system (min)	
					ISO 834 fire	Hydrocarbon fire	ISO 834 fire	Hydrocarbon fire
Composite girder CG1		1	3		35	11	35	11
		1	5	Deflection limit (L/30=113 mm)	35	11	35	11
		2	3		39	13	39	13
		2	5	39	13	39	13	
Composite girder CG2	The 1 st span			Deflection limit (L/30=80 mm)	No failure	No failure		
	Hogging moment zone	1	3	Buckling in web and bottom flange	50	24	50	24
	The 2 nd span			Deflection limit (L/30=67 mm)	68	27		
	The 1 st span			Deflection limit (L/30=80 mm)	No failure	No failure		
	Hogging moment zone	1	5	Buckling in web and bottom flange	50	24	50	24
	The 2 nd span			Deflection limit (L/30=67 mm)	68	27		
	The 1 st span			Deflection limit (L/30=80 mm)	No failure	No failure		
	Hogging moment zone	2	3	Buckling in web and bottom flange	58	28	58	28
	The 2 nd span			Deflection limit (L/30=67 mm)	75	29		
	The 1 st span			Deflection limit (L/30=80 mm)	No failure	No failure		
	Hogging moment zone	2	5	Buckling in web and bottom flange	58	28	58	28
	The 2 nd span			Deflection limit (L/30=67 mm)	75	29		

applied to solve relevant equations (Zhang *et al.* 2017). Resulting deflections were checked against the limiting values to assess the failure state of the composite girder at that time step. The time increments continued until failure occurred in the composite girder, under any of the limiting values in deflection.

5. Modal validation

The model was validated by comparing predictions from the analysis with measured response parameters in fire tests. The validation process included comparison of both thermal and structural response parameters, from the analysis with measured data in fire tests.

As part of thermal validation, temperatures within girder section at selected points, including bottom flange, mid-depth of the web, top flange, and mid-depth of the concrete slab, were compared against corresponding temperatures measured in fire tests. Fig. 13 shows a comparison of predicted temperatures within composite girder CG1 and CG2 respectively with those measured in the fire test. Overall, the predicted temperatures from the analysis agree well with measured data from the test. The slight differences in temperatures can be attributed to variations in heat transfer parameters and non-uniformity in furnace temperature, such as emissivity and convection coefficients, used in the analysis as compared with the actual conditions presented during test (furnace).

The comparison of deflections at selected locations of the girder predicted by ANSYS model and those measured in the test are shown in Fig. 14. It can be seen that ANSYS model can predict the failure time with a good acceptability. The predicted failure time of ANSYS model in the composite girders CG1 and CG2 was 32 min and 45 min respectively. There is a slight variation between the measured and predicted deflections in the composite box girders during fire exposure. This can be attributed to the idealization of stress-strain relations of steel and concrete adopted in analysis. Also, bending buckling in the web and bottom flange in the hogging moment zone dominated the fire resistance of the composite box girder CG2 at failure stage. Overall, the comparison shows a very good qualitative and quantitative agreement with the reported test data.

To better illustrate the failure state, a V-shape deformation of composite girder CG1 at failure time is shown in Fig. 15(a). It can be seen from Fig. 15(a) that the failure shape shows a good qualitative agreement with observed state in the test (Fig. 9(a)). Fig. 15(b) shows a significant buckling in the web and bottom flange in the hogging moment zone at final failure stage, which compare well with observed failure mode in fire test (Fig. 9(b)).

6. Parametric studies

Different stiffeners and fire scenarios, namely transverse and longitudinal stiffeners and ISO 834 (ISO 1999) and

hydrocarbon fire (ASTM 2014), were introduced to investigate fire resistance of the composite box bridge girders.

The composite box girders stiffened with different transverse and longitudinal stiffeners were illustrated in Fig. 16. The transverse stiffeners were designed with equal spacing along the span length, and the longitudinal stiffeners were designed with equal spacing along the web depth and the bottom flange width. Two transverse stiffeners were symmetrically set with distance of 0.2 m on the top of pier in the composite box girder CG2. All the stiffeners have the same thickness of 5 mm. m_{t0} and n_{t0} represent the number of the transverse and longitudinal stiffeners respectively, in which m_{t0} is required to greater than or equal to 3 in the design of realistic bridge girders.

A study of the parameters, which includes failure time and failure modes, is summarized in Table 4. It is concluded from the analysis that the failure time of composite box bridge girders is highly influenced by the present of longitudinal stiffeners and level of fire severity in realistic bridge fires.

Longitudinal stiffeners can highly enhance fire resistance of simply composite box bridge girders, which is due to the fact that longitudinal stiffeners can significantly increase the bending capacity.

Longitudinal stiffeners can highly enhance fire resistance of continuous composite box bridge girders. This is mainly contributed to the fact that longitudinal stiffeners can significantly resist the bending buckling in the hogging moment zone.

With closer spacing of longitudinal transverse, the continuous composite box bridge girder has better fire resistance than the simply composite box bridge girder when exposed to higher fire intensities. This is due to the fact that the longitudinal stiffeners in the web and bottom flange have more contribution to resist bending buckling in the hogging moment zone than increase the flexural rigidity in positive moment zone.

Hence, closer spacing of longitudinal stiffeners can enhance fire resistance of composite box bridge girders. However, the increase of transverse stiffeners has little influence on fire resistance of composite box bridge girders.

7. Conclusions

Based on the results from the fire tests and numerical analysis, the following conclusions can be drawn on the response of composite bridge girder exposed to localized fire.

- A measurement method based on comparative rate of deflection is provided to predict successfully the failure time in the hogging moment zone of continuous box bridge girders under certain localized fire exposure conditions.
- Under certain localized fire exposure conditions, continuous composited girders experience significantly bending buckling in the web and bottom flange in the hogging moment zone leading to formation of plastic hinge at the pier-top at failure stage.
- Failure of simply supported composite bridge girders under certain localized fire condition occurs through

deflection limit state. Whereas, deflection based criterion may not be reliable for evaluating failure of fire exposed two-span continuous composite box bridge girder. This is mainly due to that the bending buckling of the web and bottom flange in the hogging moment dominates fire resistance of continuous composite box bridge girders.

- Closer spacing of longitudinal stiffeners in the web and bottom flange can enhance fire resistance of composite box bridge girders. However, the increase of transverse stiffeners has no significant effect on fire resistance of composite box bridge girders. Thus, decreasing spacing of longitudinal stiffeners can mitigate fire hazard on most critical composite box bridges.

- Fire resistance of continuous composite box bridge girders is highly influenced by type of fire exposure and the associated fire severity. The continuous composite box bridge girders exhibit better fire resistance than the simply composite box bridge girders with closer spacing of longitudinal stiffeners and higher fire intensity.

- The proposed numerical model developed in ANSYS can successfully simulate the thermal and structural response of composite box girders under localized fire exposure conditions. The model can account for failure time and failure mode in evaluation fire resistance of composite box bridge girders.

Acknowledgments

The authors wish to acknowledge the support from Ministry of Transport of the People's Republic of China (Grant No. 2011318812970) and the support from Natural Science Foundation of China (Grant No. 51308056 and No. 51878057), National Science Basic Research Plan in Shaanxi Province of China (Grant No. 2018JM5018), Research fund for Central Universities of China (Grant No. 310821172003), Southeast University and Michigan State University. Any opinions, findings, and conclusions or recommendations expressed in this paper are those of the authors and do not necessarily reflect the views of the sponsors.

References

- Alos-Moya, J., Paya-Zaforteza, I., Garlock, M.E.M., Loma-Ossorio, E., Schiffner, D. and Hospitaler, A. (2014), "Analysis of a bridge failure due to fire using computational fluid dynamics and finite element models", *Eng. Struct.*, **68**, 96-110.
- Alos-Moya, J., Paya-Zaforteza, I., Hospitaler, A. and Rinaudo, P. (2017), "Valencia bridge fire tests: Experimental study of a composite bridge under fire", *J. Constr. Steel Res.*, **138**, 538-554.
- American Association of State Highway and Transportation Officials (AASHTO) (2007), *AASHTO LRFD Bridge Design Specifications*, 4th Edition, AASHTO, Washington, U.S.A.
- American Society for Testing and Materials (ASTM) (2014), *Standard Test Methods for Determining Effects of Large Hydrocarbon Pool Fire on Structural Members and Assemblies*, ASTM E1529-14a, West Conshohocken, Pennsylvania, U.S.A.
- ANSYS (2013), *ANSYS Metaphysics (Version 14.5)*, ANSYS Inc., Canonsburg, Pennsylvania, U.S.A.

- Aziz, E., Kodur, V.K.R., Glassman, J.D. and Garlock, M.E.M. (2015), "Behavior of steel bridge girders under fire conditions", *J. Constr. Steel Res.*, **106**, 11-12.
- Balaji, A., Aathira, M.S., Pillai, T.M. and Nagarajan, P. (2016), "Reliability studies on RC beams exposed to fire based on is456:2000 design methods", *Struct. Eng. Mech.*, **59**(5), 853-866.
- Cheng, J. and Yao, H. (2016), "Simplified method for predicting the deflections of composite box girders", *Eng. Struct.*, **128**, 256-264.
- Erdem, H. (2017), "Predicting the moment capacity of RC slabs with insulation materials exposed to fire by ann", *Struct. Eng. Mech.*, **64**(3), 339-346.
- European Committee for Standardization (CEN) (2002), *Actions on Structures. Part 1.2 General Action-Action on Structures Exposed to Fire*, Eurocode1, Brussels, Belgium.
- European Committee for Standardization (CEN) (2004), *Design of Concrete Structures. Part 1.2 General Rules-Structural Fire design*, Eurocode 2, Brussels, Belgium.
- European Committee for Standardization (CEN) (2005), *Design of Steel Structures. Part 1.2 General Rules-Structural Fire Design*, Eurocode3, Brussels, Belgium.
- Garlock, M.E.M., Paya-Zaforteza, I., Kodur, V.K.R. and Gu, L. (2012), "Fire hazard in bridges: Review, assessment and repair strategies", *Eng. Struct.*, **35**(1), 89-98.
- GB 50917 (2013), *Code for Design of Steel and Concrete Composite Bridges*, Beijing, China.
- Glassman, J., Garlock, M.E.M., Aziz, E. and Kodur, V.K.R. (2016), "Modeling parameters for predicting the postbuckling shear strength of composite girders", *J. Constr. Steel Res.*, **121**, 136-143.
- International Standard Organization (ISO) (1999), *Fire Resistance Tests-Elements of Building Construction-Part 1: General Requirements*, ISO834, Genva, Switzerland.
- Kim, S.H., Park, S.J., Wu, J.X. and Won, J.H. (2015), "Temperature variation in steel box girders of cable-stayed bridges during construction", *J. Constr. Steel Res.*, **112**, 80-92.
- Kodur, V.K.R., Aziz, E. and Dwaikat, M. (2013), "Evaluating fire resistance of steel girders in bridges", *J. Brid. Eng.*, **18**(7), 633-643.
- Kodur, V.K.R., Aziz, E.M. and Naser, M.Z. (2017), "Strategies for enhancing fire performance of steel bridges", *Eng. Struct.*, **131**, 446-458.
- Lie, T.T. and Denham, E.M.A. (1993), "Factors affecting the fire resistance of circular hollow steel columns filled with bar-reinforced concrete", NRC-CNRC Internal Report, No. 651, Ottawa, Canada.
- Morbioli, A., Tondini, N. and Battini, J.M. (2018), "A branch-switching procedure for analyzing instability of steel structures subjected to fire", *Struct. Eng. Mech.*, **67**(6), 629-641.
- Naser, M.Z. and Kodur, V.K.R. (2015), "A probabilistic assessment for classification of bridges against fire hazard", *Fire Safety J.*, **76**, 65-73.
- National Fire Protection Association (NFPA) (2011), *Standards for Road Tunnels, Bridges, and Other Limited Access Highways*, NFPA 502, Quincy, Massachusetts, U.S.A.
- Nguyen, T.T., Tan, K.H. and Burgess, I.W. (2015), "Behaviour of composite slab-beam systems at elevated temperatures: Experimental and numerical investigation", *Eng. Struct.*, **82**, 199-213.
- Nie, J.G., Tao, M.X. and Fan, J.S. (2011), "Research on cable anchorage systems for self-anchored suspension bridges with steel box girders", *J. Brid. Eng.*, **16**(5), 633-643.
- New York State Department of Transportation (2008), *Bridge Fire Incidents in New York State*, New York State Department of Transportation, U.S.A.
- Pantousa, D. and Mistakidis, E. (2017), "Rotational capacity of pre-damaged I-section steel beams at elevated temperatures", *Steel Compos. Struct.*, **23**(1), 53-66.
- Quiel, S.E., Yokoyama, T., Bregman, L.S., Mueller, K.A. and Marjanishvili, S.M. (2015), "A streamlined framework for calculating the response of steel-supported bridges to open-air tanker truck fires", *Fire Saf. J.*, **73**, 63-65.
- Tang, C.W. (2017), "Fire resistance of high strength fiber reinforced concrete filled box columns", *Steel Compos. Struct.*, **23**(5), 611-621.
- Wang, Y.C. (1998), "Composite beams with partial fire protection", *Fire Saf. J.*, **30**(4), 315-332.
- Zhou, H.T., Li, S., Chen, L. and Zhang, C. (2018), "Fire tests on composite steel-concrete beams prestressed with external tendons", *J. Constr. Steel Res.*, **143**, 62-71.
- Zhang, G., Zhu, M.C., Kodur, V.K.R. and Li, G.Q. (2017), "Behavior of welded connections after exposure to elevated temperature", *J. Constr. Steel Res.*, **320**, 88-95.
- Zhu, W.Q., Jia, J.Q. and Zhang, J.G. (2017), "Experimental research on seismic behavior of steel reinforced high-strength concrete short columns", *Steel Compos. Struct.*, **25**(5), 603-615.
- Zhang, G., Kodur, V., Hou, W. and He, S. (2017), "Evaluating fire resistance of prestressed concrete bridge girders", *Struct. Eng. Mech.*, **62**(6), 663-674.

PL